Journal of Applied Fluid Mechanics, Vol. 9, No. 3, pp. 1035-1040, 2016.
Available online at www.jafmonline.net, ISSN 1735-3572, EISSN 1735-3645.
DOI: 10.18869/acadpub.jafm.68.228.24586

Effect of Hydrophobic Coating on Hagen-Poiseuille Flows

A. Ríos-Rodríguez, C. A. Palacios-Morales, E. Bernal, G. Ascanio and J. P. Aguayo-Vallejo†

Centro de Ciencias Aplicadas y Desarrollo Tecnológico, Universidad Nacional Autónoma de México, Circuito Exterior, Ciudad Universitaria, DF 04510, México.

†*Corresponding Author Email: pablo.aguayo@ccadet.unam.mx*

(Received January 23, 2015; accepted July 7, 2015)

ABSTRACT

The effect of a hydrophobic coating on the flow through circular pipes with Newtonian fluids has been investigated. Velocity fields inside a pipe were experimentally determined by the particle image velocimetry (PIV) technique. The test fluid presented a viscosity of about sixty times higher than water viscosity. Two glass pipe configurations were used: one uncoated and another covered with an extremely hydrophobic commercial product. Comparisons between coated and uncoated pipes were made at similar Reynolds (*Re*) numbers, all in the laminar regime (70-250). Results show that the hydrophobic effect consists in an observable slip velocity at the wall, with a reduction in shear rate near the pipe boundary. Pressure drop values were estimated from a modified Hagen-Poiseuille equation, taking into consideration the non-zero velocity at the boundary for both set of experiments, and the results show a 20% reduction in the pressure drop for the hydrophobic wall compared with the uncoated pipe case.

Keywords: Slip velocity; PIV visualization; Hagen-poiseuille equation; Drag reduction.

NOMENCLATURE

$\dot{\gamma}\|_w$	shear rate at wall (s^{-1})	r	radial position (m)
$\bar{v}$	mean velocity (m/s)	R	internal radius of the tube (m)
v_z	velocity along the z-axis (m/s)	Re	Reynolds number
D	inner diameter (m)		
Iu_s	slip velocity (m/s)	μ	dynamic viscosity (Pa s)
L	length of the tube (m)	ρ	density (kg/m^3)
Q	volumetric flow rate (m^3/s)	$\Delta P/L$	pressure drop per length unit (Pa/m)

1. INTRODUCTION

A basic assumption in fluid mechanics is the so-called no-slip boundary condition, which states that the velocity of a fluid in contact with a solid boundary equals the velocity of the solid; in other words, the fluid is attached to the surface. According to Rothstein (2010), in pressure driven laminar flows, superhydrophobic surfaces can reduce drag, producing slip lengths larger than the molecular scale. In his review work, the author focused on the micro and nano-scales attempts to produce slip. However, experimentally the slip phenomenon in laminar regime has barely received attention at least at a macroscopic scale; it seems that the research of Watanabe and co-workers (Watanabe *et al*. 1998, 1999; Watanabe and Udagawa 2001) were the first studies of drag reduction through macroscopic geometries by coating a surface with a hydrophobic material. First, Watanabe *et al*. (1998) determined the slip velocity in a 15×15×2000 mm rectangular channel for the case of highly water-repellent walls, while for the hydrophilic wall, no slip was reported. However, it is important to note that, for their experiments, the pressure drop was fixed (10.8 Pa/m), meaning that the volumetric flow rates (i.e. Reynolds numbers) were different. Two fluids were tested: tap water and a solution of 20% wt. glycerin in water. For the case of water, the mean velocities were 0.116 m/s and 0.094 m/s, for the hydrophilic and hydrophobic walls, respectively. They also reported experimental velocities for Reynolds numbers from 1000 to 1980, for the water-repellent case only. Velocity measurements were obtained using a hot film anemometer and the profile was compared to the analytical solution considering slip; experiments

showed good agreement with the analytical model.

Next, Watanabe *et al*. (1999) studied the flow in circular pipes, of 6 mm and 12 mm diameters; the fluids were tap water, and two solutions of glycerin with 20% and 30% wt in water. Their results showed slip velocity for the hydrophobic material, while no slip was considered for the regular pipe. Reported hydrophobic and hydrophilic velocity profiles (at same pressure drop) are similar but with a gap, produced by the non-zero slip, additionally, the authors reported a drag reduction of 14%. In another study, Watanabe and Udagawa (2001) continued with the flow through a pipe. Special attention was paid to the turbulence, finding that no difference could be observed for the uncoated and the water-repellent pipe in this flow regime.

Churaev *et al*. (1984) measured slippage of water and mercury on quartz capillaries of radii less than 5.8 μm. The capillaries were made hydrophobic using a solution of trimethylchlorosilane in benzene. These authors mentioned that for capillaries of a radius of less than 1 μm the mean velocity differs by 10% compared to the uncoated surface; therefore, reducing capillary radius would increase the level of slip.

Slip velocity was also measured in a rectangular microchannel (30×300 μm) by Tretheway and Meinhart (2002). The channel surface was made hydrophobic with a coat of octadecyltrichlorosilane. Velocity profiles were obtained by micron-resolution particle image velocimetry (μ-PIV) and, from their results, the gap between profiles for hydrophobic and hydrophilic surfaces could be observed, as well as the non-zero velocity near the channel wall. From theory, they concluded that only at micro- and nano- scales the slip effect can be dominant, indicating that as the separation of wall becomes larger, the dominant term in the profile is the quadratic term from the standard solution, i.e., considering no-slip boundary conditions. Rothstein (2010), based on the works of Maxwell (1879), Tolstoi (1952) and Blake (1990) confirms such conclusion, mentioning that for nearly all macroscopic flows of simple fluids the no-slip condition is accurate. However, this statement is contrary to the findings of Watanabe and co-workers, who reported slip at macroscopic devices.

The aim of this work is to experimentally analyze the effect of hydrophobic coating on the laminar flow of a Newtonian fluid through a circular macroscopic pipe as a function of the Reynolds number. As the PIV system used here is an optical non-intrusive technique, measurements were reported closer to the pipe wall in comparison with the ones presented by Watanabe *et al.* (1999). In addition, the use of a fluid with higher viscosity (about 35 times) permitted to reach lower Reynolds numbers ($Re \in [74, 254]$) than those used in Watanabe *et al.* research ($Re > 300$) and then, testing slip phenomenon at smaller velocities. Slip velocity, pressure drop and shear rate at the wall are estimated from experimental information.

2. METHODS AND MATERIALS

Figure 1 shows the experimental setup used in this work. It consists basically of a pipeline array with a transparent glass pipe of 14.1 mm inner diameter, a centrifugal pump driven by a DC motor of 248 W (1/3 hp), which speed is set from a DC controller in an open-loop mode. The flow rate was measured with an electromagnetic transmitter MC 308 C (Flow Technology, Inc.). The working fluid is a solution of glycerin (85% wt.) in water, with viscosity around 0.065 Pa·s (65 cP). The solution is pumped from a reservoir to the test section. The distance from the pump to the test section is much larger than the entrance length (200 mm) for the highest *Re* number; the entrance length was computed with Dombrowski's *et al*. (1993) correlation. Therefore, fully developed flow is obtained inside the test section.

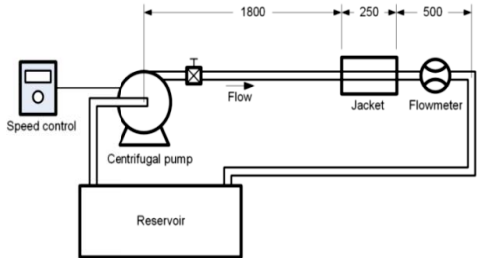

(a)

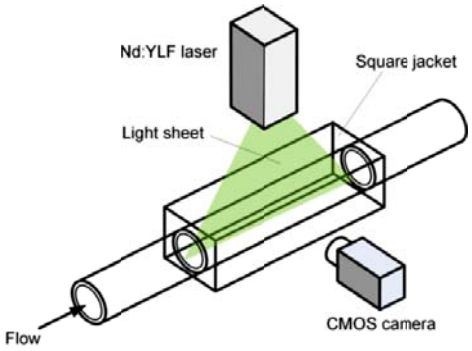

(b)

Fig. 1. Experimental setup: (a) Pipeline system (dimensions in mm); (b) PIV setup.

The 2D velocity fields were obtained using a PIV system from Dantec Dynamics. The PIV system consists of a Nd:YLF Litron laser (527 nm, 10 mJ, 1000 Hz), a Phantom high-speed camera (CMOS, 1632×1200 pixels, 11.5 μm pixel pitch, 1000 Hz) and the *Dynamic Studio* software (Dantec Dynamics). Neutrally buoyant silver-coated glass spheres with average diameter of 10 μm were used as particle tracers. The laser sheet illuminated a vertical slice aligned with the tube center and the camera was placed perpendicularly with respect to the light sheet. An adaptive cross-correlation algorithm was used to compute the velocity fields using an interrogation area of 32×16 pixels with 75% overlap obtaining a spatial resolution of

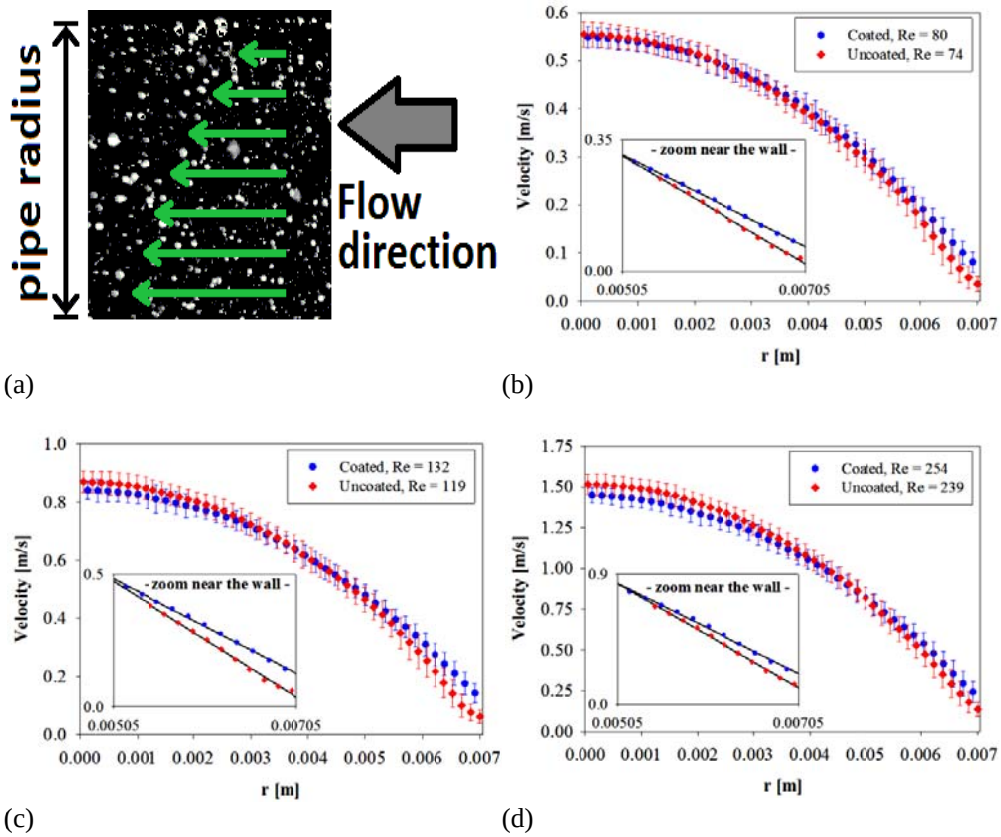

Fig. 2. Measured velocity profiles: (a) picture of the visualization with a superimposed velocity profile; (b) Results at *Re* ~ 80; (c) Results at *Re* ~ 130; (d) Results at *Re* ~ 250.

0.308×0.154 mm in the axial and radial directions respectively. The typical measurement area (velocity field) was 62.3×14.3 mm with 201×92 vectors in the axial and radial direction respectively and the sampling frequency was 200 Hz. The *peak validation* analysis (a signal-to-noise ratio identification procedure) was carried out to identify valid data; therefore, a valid vector has a signal peak (from cross correlation) consistently higher than the noise peak. After such procedure a *moving average validation* analysis was applied (Host-Madsen and McCluskey, 1994), where the average of vectors in a rectangular neighborhood are computed and compared with the analyzed point and if the deviation of the vector is high from its neighbors, the vector is rejected. In addition, the velocity profiles are first temporally averaged during 2 seconds (corresponding to 400 maps) and then, spatially averaged over 5 mm length. In the test section a square jacket containing water was used for minimizing significant changes of the refraction index as well as reducing optical distortion produced by the pipe curvature. The inner surface of the pipe was coated with a commercial highly hydrophobic film (*NeverWet™*, whose repellent top coat is based on silicones and siloxanes). For comparison purposes with slip conditions, tests were made also with a pipe having a smooth inner surface without the repellent. As the hydrophobic coating provoked large deviations in PIV measurements, a 5 mm-wide ring of the test region was left uncoated for visualization purposes only. The length of the uncoated region is small enough to prevent any significant perturbation of the flow. Assuming symmetry around the centerline, only velocities from the upper half of the pipe were measured.

3. RESULTS

Given the available experimental velocity data (40 points or more for each profile), volumetric flow rates (Q) were safely computed with the use of the trapezoidal rule. Although values displayed by the electromagnetic transmitter were in general in good agreement with the calculations, the latter ones were used for the subsequent analysis. Reynolds number is defined by $Re = \rho \bar{v}\, D/\mu$, where ρ and μ is fluid density and viscosity, respectively, D is the inner diameter and $\bar{v}$ is the mean velocity computed from experimental data. Measured velocity profiles, and the mean standard deviation for each velocity, are presented in Fig. 2, for three different flow rates. This figure also includes an image from the PIV system with a superimposed experimental velocity profile. Differences in Reynolds numbers

Table 1 Flow parameters computed from experimental data

Uncoated						Coated				
Flow rate ×10^6	Re	$\dot{\gamma}\|_w$	u_s	$\Delta P/L$		Flow rate ×10^6	Re	$\dot{\gamma}\|_w$	u_s	$\Delta P/L$
[m^3/s]	[-]	[s^{-1}]	[m/s]	[Pa/m]		[m^3/s]	[-]	[s^{-1}]	[m/s]	[Pa/m]
45.5	74	143	0.0204	2932		47.6	80	122	0.0657	2530
71.3	119	218	0.0363	4443		74.2	132	178	0.1253	3474
126.9	239	359	0.1149	6549		127.3	254	312	0.2123	5333

for any specific plot in Fig. 2 were due to the difficulty of controlling flow rates to a preset value. Some approaches to measure slip consist on determining pressure drop and flow rate and from these data, slip lengths or slip velocity are inferred (Choi *et al*. 2003; Ou *et al*. 2004; Jung and Bhushan 2010), or gather it from friction factor values (Cottin-Bizonne *et al*. 2005). Others use optical methods (as Tretheway and Meinhart 2002) to determine velocity profiles; both methods present limitations, as pointed out by Cottin-Bizonne *et al*. (2005). Here, the optical approach was followed; shear rates at wall ($\dot{\gamma}|_w$) were calculated with linear regressions of this experimental velocity (v_z) *vs.* radial position (r), for the eleven data closest to the pipe wall, located at the tube radius (R).

The criteria for choosing this number of points is because for all cases with these data, the correlation coefficient is greater than 0.999; plots for these regression lines can be observed in Figs. 2b to 2d. The slope of each regression line corresponds to the shear rate. Slip velocities (u_s) were extrapolated from these regressions, due to the fact that the PIV technique is unable to gather information exactly at the pipe boundary (Cottin-Bizonne *et al*. 2005). Note that even for the uncoated pipe, slips velocities were greater than zero, but smaller than those from the hydrophobic wall. In order to be consistent with the procedure followed here, these uncoated velocities were not forced to zero; though these non-zero values could be the result of experimental error in the measurements, most probably due to the proximity to the wall where laser reflections may interfere with the PIV system.

Table 1 contains information calculated from the experimental profiles. The first two columns on each side are the flow rate and the corresponding *Re* numbers, respectively, the third column is the shear rate at the wall, followed by the extrapolated or slip velocity and finally, a computed pressure drop ($\Delta P/L$).

To estimate the pressure drop, an expression similar to the Hagen-Poiseuille equation was derived and modified to account for the non-zero velocity at the wall. The procedure for obtaining the required relation is by solving the Navier-Stokes equation for flow through a cylindrical geometry using for the wall, the boundary condition $v_z|_{r=R} = u_s$. The resulting profile is:

$$v_z = \frac{-\Delta P\, R^2}{4\, L\, \mu}\left[1 - \left(\frac{r}{R}\right)^2\right] + u_s \qquad (1)$$

Integrating Eq. (1) over the section of the pipe and isolating the pressure drop per unit length gives:

$$\frac{-\Delta P}{L} = \frac{8\,\mu}{\pi\, R^4}[Q - \pi\, R^2\, u_s] \qquad (2)$$

It can be seen from Eq. (2) that for a fixed flow rate and viscosity, larger u_s values will reduce pressure drop linearly; however, there is not enough experimental data to find the relation between u_s and *Re*. Note that if $u_s = 0$ is set, the familiar results with the no-slip boundary are recovered.

Trends of the calculated flow parameters are easily observed in Fig. 3, where results of Table 1 are plotted.

4. CONCLUSIONS

The effect of a hydrophobic coating applied to the inner surface of the laminar flow through a circular pipe was experimentally investigated with Newtonian fluids. From the PIV data, the slip velocity, pressure drop and the shear rate were all inferred. Because the PIV technique is a non-intrusive technique, the flow was completely unaffected. Although parabolic profiles could be adjusted with correlation coefficients higher than 0.99, some deviations between this fit and the actual data were observed in the region near the wall, hence, a linear regression for data close to the pipe boundary was employed. Note that with the visualization technique used here, velocities at distances from the wall of only 0.0473 mm and 0.1291 mm, for the uncoated and coated cases, respectively, were gathered (i.e. extrapolation for slip velocities were made for very short lengths), while in the research of Watanabe's group for the flow through a pipe and according to their plots, the closest measurement was made at a distance to the wall greater than 0.5 mm.

It can be gathered from Fig. 2 that the hydrophobic effect provokes larger velocities near the pipe wall, which in turn cause that, even when the *Re* numbers are greater in all hydrophobic cases presented here, centerline velocities are slightly *lower* compared to

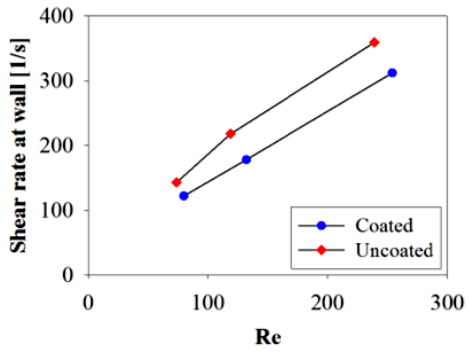

(a)

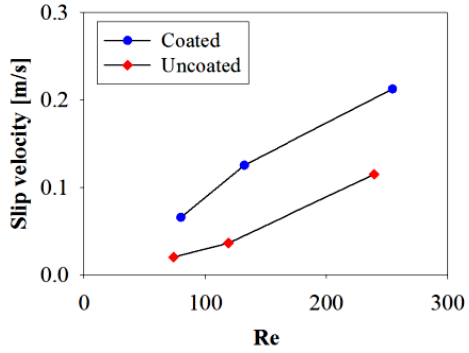

(b)

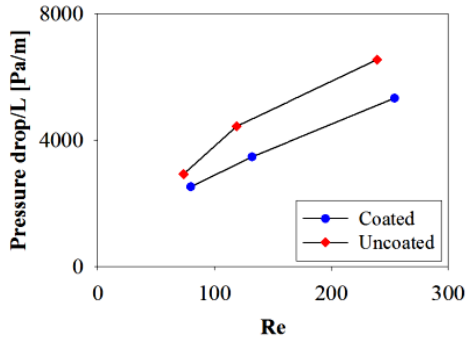

(c)

Fig. 3. Calculated flow parameters: (a) Shear rate at wall; (b) Slip velocity; (c) Pressure drop per unit length.

those for the uncoated pipe; this is evidence that slip occurs at wall, otherwise, higher velocities at centerline should have been obtained for higher *Re* numbers.

In addition, it can be seen from data in Table 1 and Fig. 3 that:

a) Larger shear rates at the boundaries are obtained for the pipe without repellent. Both trends seem to be linear.

b) Although non-zero velocities were found for the uncoated case, the slip velocities for the repellent wall are larger by a factor of 1.5 up to 3 times than those from the uncoated surface.

c) The reduction in pressure drop (or drag) for the hydrophobic case is roughly 20% compared to that for the uncoated pipe. If the velocity at the uncoated wall were assumed to be zero (common assumption for macroscopic devices), the difference in pressure drop would have been greater.

Note that Watanabe and co-workers reported a drag reduction of 14% for flow into pipes, while here a 20% is estimated. To obtain this result a much more viscous fluid was tested. Also note that even increasing the viscosity by more than 35 times, the effect in drag reduction is moderate, this seems to be consistent with trends shown in Watanabe *et al*. (1999).

In general it is observed that the hydrophobic effect is increased by increasing inertia in the flow, but only slightly.

REFERENCES

Choi, C. H., J. A. Westin and K. S. Breuer (2003). Apparent slip flows in hydrophilic and hydrophobic microchannels. *Physics of Fluids* 15, 2897-2902.

Churaev, N. V., V. D. Sobolev and A. N. Somov (1984). Slippage of liquids over lyophobic solid surfaces. *Journal of Colloid and Interface Science* 97, 574-581.

Cottin-Bizonne, C., B. Cross, A. Steinberger and E. Charlaix (2005). Boundary slip on smooth hydrophobic surfaces: Intrinsic effects and possible artifacts. *Physical Review Letters* 94, 056102.

Dombrowski, N., Foumeny, S. Ookawara and A. Riza (1993). The influence of Reynolds number on the entry length and pressure drop for laminar pipe flow. *The Canadian Journal of Chemical Engineering* 71, 472-476.

Host-Madsen, A. and D. R. McCluskey (1994). On the accuracy and reliability of PIV measurements. *7th International Symposium on Applications of Laser Techniques to Fluid Mechanics 11-14 July 1994*, Lisbon, Portugal.

Jung, Y. C. and B. Bhushan (2010). Biomimetic structures for fluid drag reduction in laminar and turbulent flows. *Journal of Physics: Condensed Matter* 22, 035104.

Ou, J., B. Perot and J. P. Rothstein (2004). Laminar drag reduction in microchannels using ultrahydrophobic surfaces. *Physics of Fluids* 16, 4635-4660.

Rothstein, J. P. (2010). Slip on superhydrophobic surfaces. *Annual Review of Fluid Mechanics* 42, 89-109.

Tretheway, D. C. and C. D. Meinhart (2002). Apparent fluid slip at hydrophobic microchannel walls. *Physics of Fluids* 14, L9-L12.

Watanabe, K. and H. Udagawa (2001). Drag

reduction of non-Newtonian fluids in a circular pipe with a highly water –repelent wall. *AIChE Journal* 47, 256-262.

Watanabe, K., Yanuar and H. Mizunuma (1998). Slip of Newtonian fluids at slid boundary. *The Japan Society of Mechanical Engineers International Journal Ser. B* 41, 525-529.

Watanabe, K., Yanuar and H. Udagawa (1999). Drag reduction of Newtonian fluid in a circular pipe with a highly water-repellent wall. *Journal of Fluid Mechanics* 381, 225-238.